Journal of Nuclear Materials 390–391 (2009) 295–298

Contents lists available at ScienceDirect

Journal of Nuclear Materials

journal homepage: www.elsevier.com/locate/jnucmat

Comparison of kinetic and fluid neutral models for attached and detached state

M. Furubayashi [a,*], K. Hoshino [b], M. Toma [a], A. Hatayama [a], D. Coster [c], R. Schneider [d], X. Bonnin [e], H. Kawashima [b], N. Asakura [b], Y. Suzuki [b]

[a] Graduate School of Science and Technology, Keio University, Hatayama Lab 25-505, 3-14-1 Hiyoshi Kohoku-ku, Yokohama Kanagawa 223-8522, Japan
[b] Naka Fusion Institute, Japan Atomic Energy Agency, 311-0193, Japan
[c] Max-Planck-Institut für Plasmaphysik, Garching, Germany
[d] Max-Planck-Institut für Plasmaphysik, Greifswald, Germany
[e] LIMHP-CNRS, Université Paris 13, Villetaneuse, France

ARTICLE INFO

PACS:
52.25.Fi
52.25.YA
52.55.Fa
52.65.−y

ABSTRACT

Neutral behavior has an important role in the transport simulations of the edge plasma. Most of the edge plasma transport codes treat neutral particles by a simple fluid model or a kinetic model. The fluid model allows faster calculations. However, the applicability of the fluid model is limited. In this study, simulation results of JT-60U from kinetic neutral model and fluid neutral model are compared under the attached and detached state, using the 2D edge plasma code package, SOLPS5.0. In the SOL region, no significant differences are observed in the upstream plasma profiles between kinetic and fluid neutral models. However, in the divertor region, large differences are observed in plasma and neutral profiles. Therefore, further optimization of the fluid neutral model should be performed. Otherwise kinetic neutral model should be used to analyze the divertor region.

1. Introduction

Neutral behavior has an important role in the transport simulations of the edge plasma. Most of the edge plasma transport codes treat neutral particles by a simple fluid model or a kinetic model. The kinetic treatments by the Monte-Carlo method are more exact compared to the fluid model. However, the kinetic neutral model introduces the issue to the Monte-Carlo noise and raises the question of proving convergence [1]. In addition, the simulation cost will be massive. On the other hand, the fluid model is easier to prove convergence, and faster than the kinetic model. However, the fluid model has a limited applicability.

The 2D edge plasma code SOLPS5.0 [2], consists of a fluid code B2.5 [3], coupled to a Monte-Carlo neutral code EIRENE [4]. There are two options in this SOLPS5.0 code package for the neutrals. One option treats the neutrals by a fluid model using B2.5 and the other by the kinetic model using EIRENE. Also the EIRENE code can be used standalone. Benchmarks of the kinetic neutral model (B2.5-EIRENE), and the fluid model (B2.5) are done in Refs. [5,6]. However, the benchmark studies of neutral model were limited to the detached case.

In this study, we compared the results from the kinetic neutral model and fluid neutral model in the detachment and attachment condition, using the 2D edge plasma code package, SOLPS5.0. To consider both detached and attached case, we changed the value of the core boundary D^+ density in a wide range.

2. Simulation model

Fig. 1 shows the overall view and a zoom-in view of the numerical mesh generated from the JT-60U MHD equilibrium. The simulation model used in this research is the same as Ref. [6].

2.1. Simulation model for plasma

In this study, fluid model is applied for plasma. The validity of the fluid treatment can be expressed by the Knudsen number:

$$K_N = \lambda/L \ll 1, \quad (1)$$

where λ is the mean free path, and L is the characteristic length of the system. To apply the fluid treatment, Knudsen number needs to be at least less than 1.

The B2.5 multi fluid code simultaneously solves the particle balance, parallel momentum balance, ion and electron energy balance and the current continuity equations. The deuterium ions, D^+, and all the carbon ions, C^+–C^{6+}, are described by the fluid approximation in B2.5. The detailed description of these basic equations and the expression for the radial and poloidal velocity components are given in Ref. [7]. The transport coefficients are chosen based on

* Corresponding author.
E-mail addresses: akh@appi.ppl.keio.ac.jp, mfuru@ppl.appi.keio.ac.jp (M. Furubayashi).

0022-3115/$ - see front matter © 2009 Published by Elsevier B.V.
doi:10.1016/j.jnucmat.2009.01.127

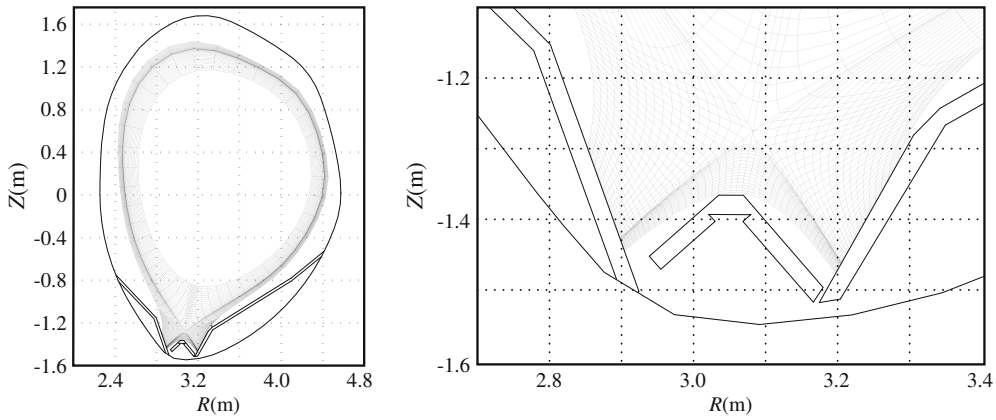

(a) Overall View (b) Zoom-in View

Fig. 1. The JT-60U geometrical configuration. (a) Numerical grid for the analysis and the vacuum vessel and (b) zoom-in view of the divertor region.

the comparison between the simulation results and the experimental data in the previous study [8].

The boundary conditions are as follows: at the core boundary the D^+ density is specified, and the total energy input is equally split between ion and electron channels. The net particle fluxes across the core boundary are assumed to be zero for all the ion species. The Bohm-criterion is assumed at the divertor plate, to obtain the monotonic potential drop across the sheath. For the boundary condition at the wall-side, a radial decay length of 1 cm for the temperature of ions and electrons is used. Also for the wall-side, the leakage option is used for the density. Here, the particle fluxes for each kind of particles are given by a leakage factor of α in the following equation.

$$\Gamma = \alpha C_s n_a, \tag{2}$$

where C_s is the ion sound velocity, and n_a is the density of each particles.

2.2. Kinetic neutral model

In the kinetic neutral model, Monte-Carlo neutral code, EIRENE, is coupled to B2.5. The B2.5 code treats ions and EIRENE treats the neutrals. The EIRENE code directly solves the Boltzmann transport equation by using the Monte-Carlo method to determine the distribution function of neutrals. The neutral species D, D_2, and C are treated by EIRENE. The EIRENE code can take into account important atomic and molecular processes [4,8], such as electron impact ionization, elastic collisions, charge exchange, dissociation, dissociative ionization, and recombination.

2.3. Fluid neutral model

In the fluid neutral model, the neutral species, D and C, are treated by B2.5, just like ion species using the same equations without electromagnetic terms. Although the atomic and molecular processes [9] are very important for the neutral dynamics in the divertor region, the molecules are not considered in the present model. Also neutrals are assumed to have the same common temperature as all other ion species. The pressure-driven diffusion flux for the neutral is given by the following equation.

$$\Gamma = -D_n^p \nabla p_n \quad D_n^p = \frac{v_{th,n}^2}{(K_{CX} n_i + K_{ion} n_e) T_n}, \tag{3}$$

where n_{sep} is the density of plasma at the outer-midplane separatrix, $v_{th,n}$ is the neutral thermal velocity, T_n is the neutral temperature shared with ions, n_i and n_e are the density of ion and electron, and K_{CX} and K_{ion} are the rate coefficients for the charge exchange and ionization.

Some parameters used in the fluid model are changed from the kinetic neutral model to fit the mid-plane profiles. Following recommendations from Ref. [5] are used to fit the mid-plane profiles: (1) use the core neutral loss boundary condition rather than the zero flux boundary condition, (2) use a neutral flux limiter. To apply the fluid model to the neutrals, the neutral mean free path needs to be smaller than plasma and neutral gradient length, i.e., Eq. (1) should be satisfied also for the neutrals. However, this condition is not satisfied for neutrals in the divertor region. Therefore, some correction for the kinetic effects, i.e., a neutral flux limiter is included in the model. In this calculation of the fluid neutral model, the neutral particle flux Γ is limited to Γ_{free}:

$$\Gamma_{free} = \frac{1}{4} n_n \bar{v}, \tag{4}$$

by the following equation.

$$\Gamma' = \frac{\Gamma}{\sqrt{1 + (\Gamma/\Gamma_{free})^2}}, \tag{5}$$

where n_n is the density of the neutrals, $\bar{v}$ is the average speed, and Γ' is the neutral particle flux corrected by the kinetic effect.

Also for the fluid neutral model, the feedback boundary condition [6] is used at the wall-side to fit the upstream profiles. This boundary condition adjusts the incoming neutral flux from the wall, to fix the value of the electron density at the separatrix in the outer-midplane.

3. Results

In this calculation, we set the value of the total energy input to 2.5 MW, and leakage factor $\alpha = 10^{-3}$. The values of 1.0–$3.6 \times 10^{19}\,m^{-3}$ are used for the D^+ density at the core interface boundary, to attain the attachment and detachment conditions. We have done a simulation for the following three models: 'Model A' fluid neutral model (B2.5), 'Model B' kinetic neutral model with its own self consistent background plasma (B2.5-EIRENE), and 'Model C' kinetic neutral model using the background plasma profiles from model A (EIRENE). We focused on the profiles at the outer diverter plate and compared the results from these models.

3.1. Electron temperature

Fig. 2 shows the radial profiles of electron temperature at the outer divertor plate from the model A and model B. When the D^+

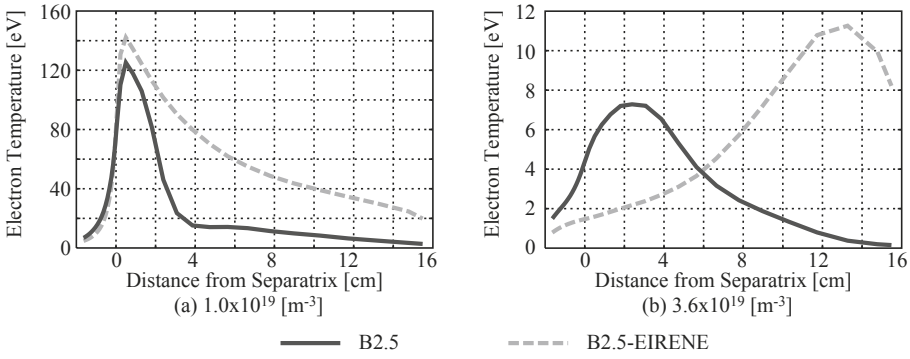

Fig. 2. Electron temperature at divertor plate. With the core D^+ density of (a) 1.0×10^{19} m^{-3}, and (b) 3.6×10^{19} m^{-3}.

density at the core boundary is low, the results from model B model and model A are both in the attached condition. When the core D^+ density is high, model B is in the detached state with the electron temperature at the separatrix being lower than 5 eV. The result from model A has a peak near the strike point, while model B has a peak at the outer-side of the strike point. In experiments [10], a peak is recognized outside of the strike point, in the radial profile of electron temperature at the divertor plate. In model B, the power dissipation by the radiation mainly by carbon is observed in the divertor region along the separatrix to the strike point. Therefore, the radiation may be the possible cause of the temperature decrease near the separatrix, making it easier to detach. Therefore, detailed study of sputtering and impurity transport may be necessary in the near future.

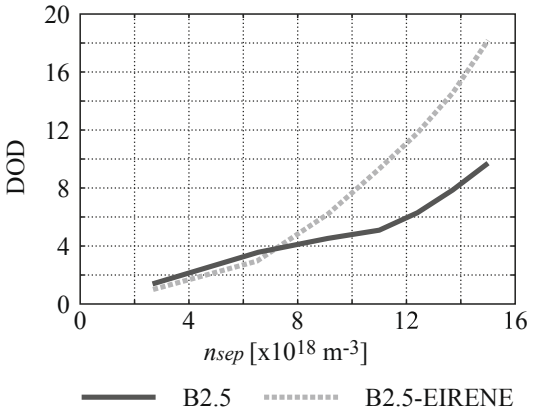

Fig. 3. Degree of detachment.

The detachment can also be identified by the degree of detachment (DOD) plot [11]. The DOD is determined by the following equation,

$$\mathrm{DOD} = C n_{sep}^2 / \Gamma_d, \tag{6}$$

where n_{sep} is the density of plasma at the outer-midplane separatrix, Γ_d is the plasma particle flux toward the outer target, and C is the normalization coefficient. Fig. 3 shows the DOD plot from model A and B. Here we can also see that the case B is easier to detach.

3.2. Neutral profiles

Next we focused on the density profile of neutrals (deuterium atoms and molecules). Fig. 4 shows the radial profiles of neutral density just in front of the outer divertor plate, i.e., neutral densities are plotted as a function of the distance d from the separatrix along the target plate. The results from model A, B, and C are compared. As seen from Fig. 4, the density profiles have a similar tendency for the most part of the radial extent. The result from model A, however, is considerably different from those by model B and C, both in the private region ($d < 0$) and outer region of the target plate near the wall-side boundary. In these regions, neutral density from model A increases, while model B and C decreases.

To understand above characteristics of the neutral density, the following fluxes are plotted in Fig. 5. Fig. 5 shows the radial particle flux of neutrals at the divertor plate, calculated from Eq. (3): (pressure-driven particle flux), Eq. (4): (free particle flux), and Eq. (5): (particle flux limited by the flux limiter). In fact, the ratio of the diffusion flux Γ to the free streaming flux Γ_{free}, roughly becomes the Knudsen number as follows:

$$K_N \approx |\Gamma/\Gamma_{free}| \propto \lambda/L. \tag{7}$$

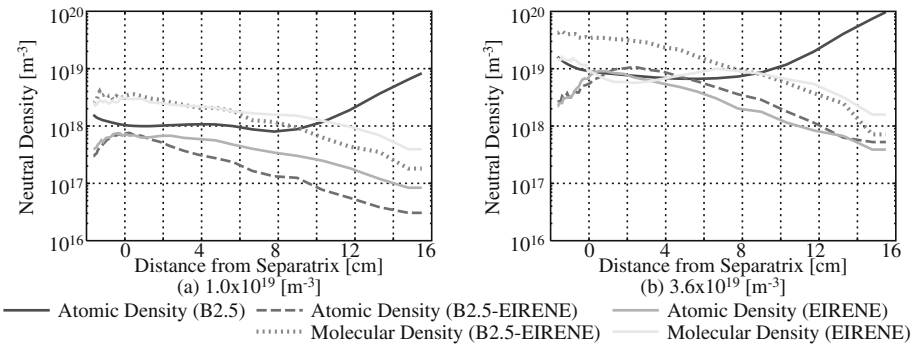

Fig. 4. Neutral density at divertor plate. With the core D^+ density of (a) 1.0×10^{19} m^{-3}, and (b) 3.6×10^{19} m^{-3}.

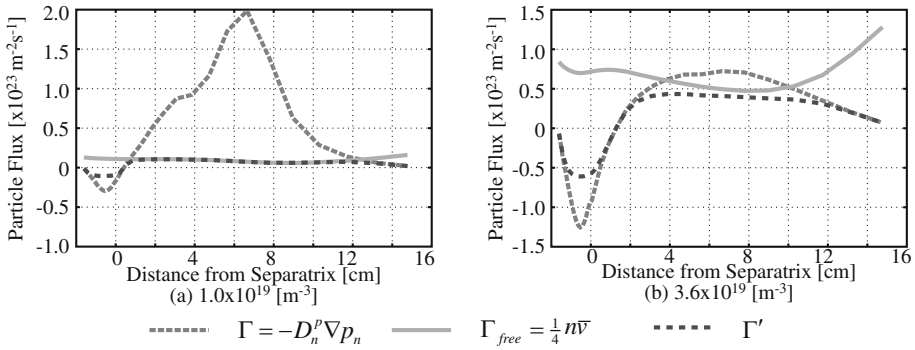

Fig. 5. Neutral particle flux in the radial direction at the divertor plate, calculated from $\Gamma = -D_n^p \nabla p_n$, $\Gamma_{free} = \frac{1}{4} n\bar{v}$, and Γ'. With the core D^+ density of (a) 1.0×10^{19} m^{-3}, and (b) 3.6×10^{19} m^{-3}.

From this relation, if Γ becomes larger than Γ_{free}, Knudsen number becomes very large. Then the fluid model can not be applicable in such region without the kinetic correction. As seen from Fig. 5(a), $|\Gamma/\Gamma_{free}| \gg 1$ in most of the radial extent in the attached case. Even in the detached case, Γ is larger than Γ_{free} and the condition $K_N \ll 1$ is violated in most of radial extent. In the present model, however, the kinetic effect is taken into account by introducing the flux limiter and the flux becomes Γ_{free} from Eq. (5), if $|\Gamma/\Gamma_{free}| \gg 1$. Indeed, in Fig. 5, the flux from model A is almost equal to the free streaming flux in most of radial extent.

The increase of the neutral density in the both end of the target, from model A can also be explained by the particle flux. In this calculation, the particle flux of neutrals leaking out of the boundary is set to a small value by the leakage factor $\alpha = 10^{-3}$, at the wall-side boundary. Therefore, from Eq. (3), the neutral pressure profile at the divertor plate is forced to be a small value at the both edge of the target. In model A, the neutral temperature (which is assumed to be the same as the ion temperature) decreases towards the both inner and outer end of the outer target. Therefore, the neutral density needs to increase to keep the pressure profile constant. In the fluid neutral model, the ion temperature is also used for neutral temperature, assuming that the charge exchange occurs frequently. However, in the divertor region, the neutral mean free path of the charge exchange is still relatively large. Therefore, the value of neutral and ion temperature does not always become the same. Thus, we may need to reconsider the assumption that the neutral temperature is the same as the ion temperature.

4. Summary and future study

Kinetic neutral model and fluid neutral model have been applied to the wide range of upstream density. To compare divertor plasma and neutral characteristics, the upstream profiles are carefully fitted.

The profiles of electron temperature and DOD plot have been compared between the kinetic and fluid neutral model. In addition, neutral density profiles have been compared between the fluid neutral model and kinetic neutral model. The applicable condition ($K_N \ll 1$) of fluid neutral model is easily violated in the divertor region. Therefore, the kinetic model or the fluid model with the kinetic correction is indispensable to mach the results. Moreover, the neutral densities in the private region and outer boundary region near the wall-side the boundary are shown to be sensitive to the boundary condition for the radial neutral flux at these boundary, and also sensitive to the assumption of the neutral temperatures.

From this benchmark study, further improvement or optimization of fluid neutral model, ex. (1) the boundary condition, and (2) the assumption of the neutral temperature, should be made to reproduce the reasonable divertor characteristics. Otherwise the kinetic model should be used for neutrals to analyze the divertor region.

References

[1] D. Reiter et al., Fus. Sci. Technol. 47 (2005) 172.
[2] R. Schneider et al., Contrib. Plasma Phys. 46 (2006) 3.
[3] V. Rozhansky et al., J. Nucl. Mater. 41 (2001) 387.
[4] D. Reiter et al., J. Nucl. Mater. 220–222 (1995) 987.
[5] D. Coster et al., Phys. Scr. T 108 (2004) 7.
[6] K. Hoshino et al., Contrib. Plasma Phys. 48 (2008) 136.
[7] V. Rozhansky et al., Contrib. Plasma Phys. 41 (2001) 328.
[8] A. Hatayama et al., Nucl. Fus. 40 (2000) 2009.
[9] R. Maingi et al., Nucl. Fus. 34 (1994) 283.
[10] N. Asakura et al., Nucl. Fus. 44 (2004) 503.
[11] P.C. Stangby, The Plasma Boundary of Magnetic Fusion Devices, Institute of Publishing, Bristol, 2000 (Chapter 5).